

# QCD at non-zero temperature: bulk properties and heavy quarks

Péter Petreczky

Physics Department Brookhaven National Laboratory Upton, NY, 11973, USA

**Abstract:** I review recent progress in lattice QCD at non-zero temperature with emphasis on the calculations of equation of state and the properties of heavy quark anti-quark pairs at high temperatures. I also briefly discuss the deconfinement and chiral symmetry restoring aspects of the QCD transition at finite temperature

## 1 Introduction

It is expected that strongly interacting matter undergoes a transition in some temperature interval from hadron gas to deconfined state also called the quark gluon plasma (QGP) [1]. Creating deconfined medium in a laboratory is the subject of the large experimental program at RHIC [2] and is going to be the goal of the future heavy-ion program at LHC [3]. Attempts to study QCD thermodynamics on the lattice go back to the early 80's when lattice calculations in  $SU(2)$  gauge theory provided the first rigorous theoretical evidence for deconfinement [4, 5, 6]. The problem of calculating thermodynamic observables in pure gluonic theory was solved in 1996 [7], while calculation involving dynamical quarks were limited to large quark masses and had no control over discretization errors [8, 9, 10] (see Refs. [11, 12] for reviews). Lattice calculations of QCD thermodynamics with light dynamical quarks remained challenging until recently. During the past 5 years calculations with light  $u, d$  quarks have been performed using improved staggered fermion actions [13, 14, 15, 16, 17, 18, 19, 20, 21, 22, 23, 24] (see Refs. [26, 27].)

To get reliable predictions from lattice QCD the lattice spacing  $a$  should be sufficiently small relative to the typical QCD scale, i.e.  $\Lambda_{QCD}a \ll 1$ . For staggered fermions, which are used for calculations at non-zero temperature, discretization errors go like  $\mathcal{O}((a\Lambda_{QCD})^2)$  but discretization errors due to flavor symmetry breaking turn out to be numerically quite large. To reduce these errors one has to use improved staggered fermion actions with so-called fat links [30]. At high temperature the dominant discretization errors go like  $(aT)^2$  and therefore could be very large. Thus it is mandatory to use improved discretization schemes, which improve the quark dispersion relation and eliminate these discretization errors. Lattice fermion actions used in numerical calculations typically implement some version of fat links as well as improvement of quark dispersion relation and are referred to as  $p4$ ,  $asqtad$ ,  $HISQ$  and  $stout$ . In lattice calculations the temperature is varied by varying the lattice spacing at fixed value of the temporal extent  $N_\tau$ . The temperature  $T$  is related to lattice spacing and temporal extent,  $T = 1/(N_\tau a)$ . Therefore taking the continuum limit corresponds to  $N_\tau \rightarrow \infty$  at the fixed physical volume. For the same reason discretization errors in the hadronic phase could be large when the temperature  $T$  is small.

In this paper I am going to discuss lattice QCD calculation of the transition temperature, equation of state as well as different spatial and temporal correlation functions relevant for phenomenology of heavy quarks.

## 2 Equation of State

The equation of state has been calculated with  $p4$  and  $asqtad$  action on lattices with temporal extent  $N_\tau = 4, 6$  and  $8$  [17, 18, 20]. In these calculations the strange quark mass was fixed to its physical value, while the light ( $u, d$ ) quark masses 10 times smaller than the strange quark mass have been used. These correspond to pion masses of  $(220 - 260)$  MeV. The calculation of thermodynamic observables proceeds through the calculation of the trace of the energy momentum tensor  $\epsilon - 3p$  also known as trace anomaly or interaction measure. This is due to the fact that this quantity can be expressed in terms of expectation values of local gluonic and fermionic operators. The explicit expression for  $\epsilon - 3p$  in terms of these operators for  $p4$  and  $asqtad$  actions can be found in Ref. [20]. Different thermodynamic observables can be obtained from the interaction measure through integration. The pressure can be written as

$$\frac{p(T)}{T^4} - \frac{p(T_0)}{T_0^4} = \int_{T_0}^T \frac{dT'}{T'^5} (\epsilon - 3p). \quad (1)$$

The lower integration limit  $T_0$  is chosen such that the pressure is exponentially small there. Furthermore, the entropy density can be written as  $s = (\epsilon + p)/T$ . Since the interaction measure is the basic thermodynamic observable in the lattice calculations it is worth discussing its properties more in detail. In Fig. 1 I show the interaction measure for  $p4$  and  $asqtad$  actions for two different lattice spacings corresponding to  $N_\tau = 6$  and  $8$ . In the high temperature region,  $T > 250$  MeV results obtained with two different lattice spacings and two different actions agree quite well with each other. Furthermore, recent calculations with HISQ actions also give results for the trace anomaly which are consistent with these [24]. Discretization errors are visible in the temperature region, where  $\epsilon - 3p$  is close to its maximum as well as in the low temperature region. At low temperatures the lattice data have been compared with the hadron resonance gas (HRG). As one can see the lattice data fall below the resonance gas value. This is partly due to the fact that the light quark masses are still about two times larger than the physical value as well as to discretization errors. The  $\mathcal{O}((a\Lambda_{QCD})^2)$  discretization errors in the hadron spectrum are suppressed at high temperatures as the lattice spacing  $a$  is small there. Also hadrons are not the relevant degrees of freedom in this temperature region. But at small temperatures, where hadrons are the relevant degrees of freedom, these discretization effects are significant. It turns out, however, that the HRG model that takes into account the quark mass dependence and discretization errors in the hadron spectrum can describe the lattice data quite well [31, 32]. The large discretization errors in the low temperature region is the reason for the discrepancies with the stout results at temperatures  $T < 200$  MeV [23]. The lattice results for the trace anomaly obtained with stout action are also different in the high temperature limit [23]. Namely,  $(\epsilon - 3p)/T^4$  calculated with stout action is about 50% smaller in the high temperature region. To resolve this problem calculation at finer lattice spacing are needed.

The pressure, the energy density and the entropy density are shown in Fig. 2. The energy density shows a rapid rise in the temperature region  $(185 - 195)$  MeV and quickly approaches about 90% of the ideal gas value. The pressure rises less rapidly but at the highest temperature it is also only about 15% below the ideal gas value. In the previous

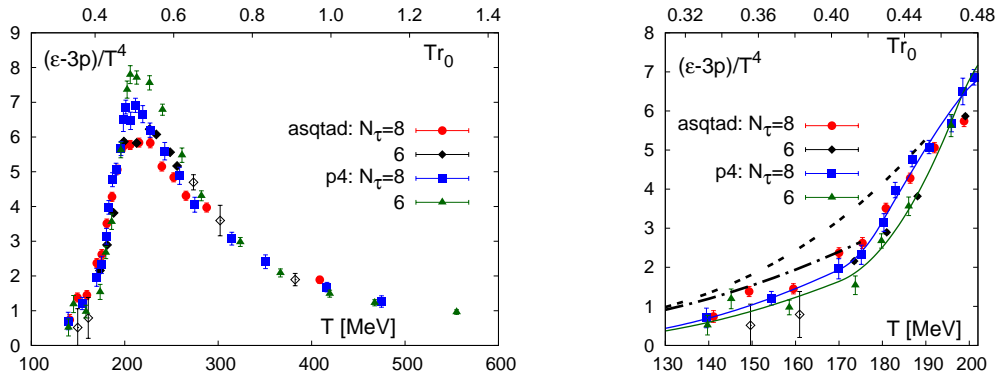


Figure 1: The interaction measure calculated with  $p4$  and  $asqtad$  actions in entire temperature range (left) and at low temperatures (right) from Ref. [20]. The dashed and dashed-dotted lines are the prediction of hadron resonance gas (HRG) with all resonances included up 2.5GeV (dashed) and 1.5GeV (dashed-dotted), respectively.

calculations with the  $p4$  action it was found that the pressure and energy density are below the ideal gas value by about 25% at high temperatures [10]. Possible reason for this larger deviation could be the fact that the quark masses used in this calculation were fixed in units of temperature instead being tuned to give constant meson masses as lattice spacing is decreased. As discussed in Ref. [41] this could reduce the pressure by 10 – 15% at high temperatures. In Fig. 2 I also show the entropy density divided by the corresponding ideal gas value and compare the results of lattice calculations with resummed perturbative calculation [33, 34] as well as with the predictions from AdS/CFT correspondence for the strongly coupled regime [35]. The later is considerably below the lattice results. Note that pressure, energy density and the trace anomaly have also been recently discussed in the framework of resummed perturbative calculations which seem to agree with lattice data quite well [36].

The differences between the *stout* action and the  $p4$  and  $asqtad$  actions for the trace anomaly translates into the differences in the pressure and the energy density. In particular, the energy density is about 20% below the ideal gas limit for the *stout* action.

### 3 Fluctuations of conserved charges

The pressure at non-zero chemical potentials can be evaluated using Taylor expansion. The Taylor expansion can be set up in terms of quark chemical potentials or in terms of chemical potentials corresponding to baryon number  $B$ , electric charge  $Q$  and strangeness  $S$  of hadrons. The expansion coefficients in quark chemical potential  $\chi_{uds}^{jkl}$  and the hadronic ones  $\chi_{BQS}^{jkl}$  are related to each other. For a more detailed discussion on this see Ref. [37]. Taylor expansion can be used to study the physics at non-zero baryon density. However, the expansion coefficients also give important information about fluctuation of conserved charges, which turn out to be sensitive probes of deconfinement and chiral symmetry restoration. Fluctuations of conserved charges have been studied

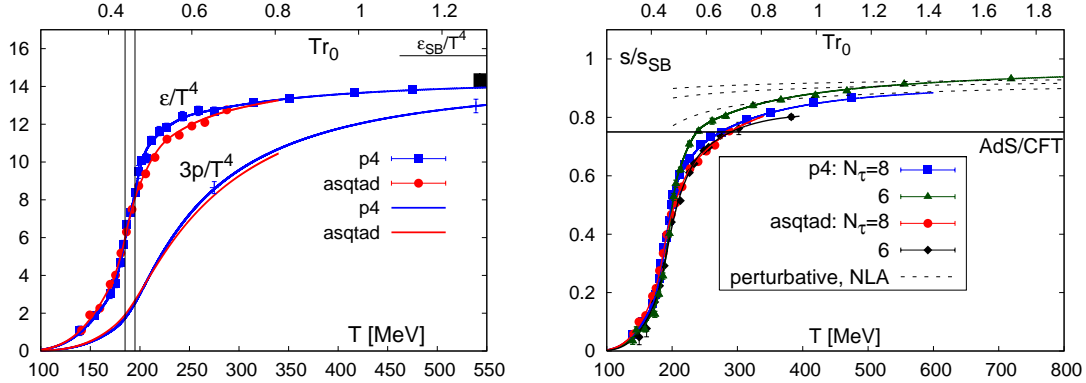


Figure 2: The energy density and the pressure as function of the temperature (left), and the entropy density divided by the corresponding ideal gas value (right). The dashed lines in the right panel correspond to the resummed perturbative calculations while the solid black line is the AdS/CFT result.

in detail using *asqtad* and *p4* actions [13, 20, 37]. In Fig. 3 I show the quadratic and quartic fluctuations of  $B$ ,  $Q$  and  $S$ . Fluctuations are suppressed at low temperatures because conserved charges are carried by massive hadrons, but rapidly grow in the transition region  $T = (185 - 195)$  MeV as consequence of deconfinement. At temperatures  $T > 300$  MeV fluctuations are reasonably well described by ideal gas of quarks. Quartic fluctuations exhibit a peak near the transition region, which at sufficiently small quark masses can be related to the chiral transition and the corresponding critical exponents (see discussion in Refs. [20]). As one can see from the figure quadratic fluctuations show visible cutoff dependence at low temperatures, while the cutoff dependence is small for  $T > 250$  MeV.

The transition from hadronic to quark degrees of freedom can be particularly well seen in the temperature dependence of the Kurtosis, which is the ratio of quartic to quadratic fluctuations. This quantity can be also measured experimentally. In Fig. 4 I show the Kurtosis of the baryon number as a function of the temperature. At low temperatures it is temperature independent and is close to unity in agreement with the prediction of the hadron resonance gas model. In the transition region it sharply drops from the hadron resonance gas value to the value corresponding to an ideal gas of quarks. Since the fluctuations of conserved charges are so well described by ideal quark gas it is interesting to compare the lattice results for quark number fluctuations with resummed perturbation theory. Quadratic quark number fluctuations are also called quark number susceptibilities and have been calculated in resummed perturbation theory [38, 39, 40]. The comparison of the resummed perturbative results with lattice calculations performed with *p4* action [42] for the quark number susceptibility divided by the ideal gas value is shown in Fig. 4. The figure shows a very good agreement between the lattice calculations and resummed perturbative results. It is also interesting to compare findings of the lattice calculations with the results obtained in strongly coupled gauge theories using AdS/CFT correspondence. The result from AdS/CFT calculations shown in the figure

as the solid black line is significantly below the lattice results <sup>1</sup>. Let me finally note that the discretization errors in the lattice calculations of the fluctuations are small at high temperatures when calculated with the  $p_4$  action. The same is true for *asqtad* action [13, 20].

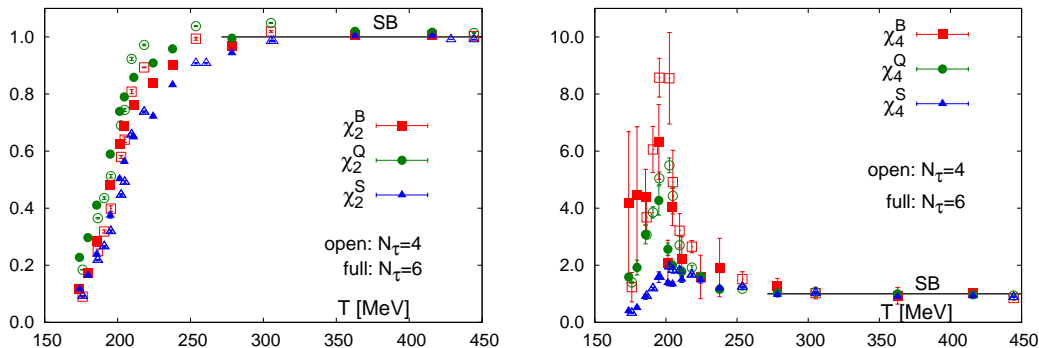


Figure 3: The quadratic (left) and quartic (right) fluctuations of  $B$ ,  $Q$  and  $S$  as function of the temperature [37]. The open symbols correspond to the results obtained on  $N_\tau = 4$  lattices, while the filled symbols to the ones obtained on  $N_\tau = 6$  lattices.

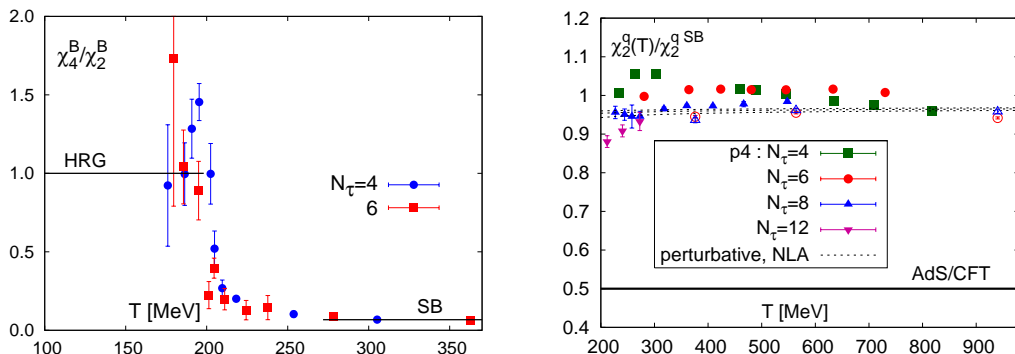


Figure 4: The Kurtosis of baryon number (left) and the quark susceptibility compared with resummed perturbative calculations (right). The open symbols on the right plot correspond to *asqtad* results for strange quark number susceptibility [13]. The resummed perturbative results were obtained in next-to-leading approximation (NLA) [39].

## 4 Chiral and deconfinement transition

The finite temperature transition in QCD has aspects related to deconfinement and chiral symmetry restoration. Deconfinement aspects of the transition are related to color screening and, for infinitely heavy quarks, also to the center symmetry. The order parameter for deconfinement is the Polyakov loop which is related to the free energy of isolated static quark. The breaking of the center symmetry is signaled by non-zero value of the Polyakov loop. In the opposite limit of massless quarks QCD has the chiral symmetry.

<sup>1</sup>the conserved charges considered in these calculations are not exactly the quark numbers, see discussion in Ref. [26].

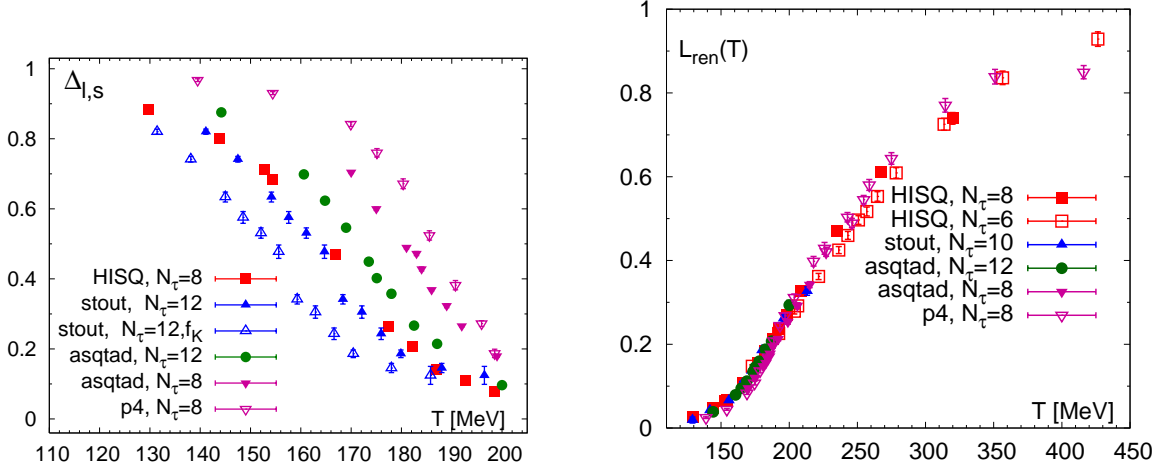


Figure 5: The subtracted chiral condensate (left) and the renormalized Polyakov loop (right) calculated for different actions [19, 21, 24].

The quark condensate  $\langle \bar{\psi}\psi \rangle$  is the order parameter for this symmetry. The chiral symmetry is broken in the vacuum and expected to be restored at high temperatures. In Fig. 5 the renormalized Polyakov loop and the subtracted chiral condensate are shown. Both quantities show a smooth change in the transition region which is consistent with the fact that the finite temperature transition is an analytic crossover and not a true phase transition [43]. It is not clear to what extent the center symmetry is relevant for the physical values of the quark masses and it is difficult to define a deconfinement transition temperature. The universal aspects of the chiral transition seem to be relevant for the range of quark masses which include the physical light quark mass and the corresponding transition temperature can be defined. Calculations with the p4 action on  $N_\tau = 4$  and 6 lattices gave an estimate  $T_c = 192(4)(7)\text{MeV}$  for the chiral transition temperature [15] which is significantly larger than the value of about  $155\text{MeV}$  obtained for stout action. This is due to large flavor symmetry breaking for the p4 action. As one can see from Fig. 5 the discrepancies between different actions are reduced when considering larger  $N_\tau$  or the HISQ action where the effects of flavor symmetry breaking are much smaller. It is expected that all actions will give the same result in the continuum limit resulting in a transition temperature of  $(150 - 160)\text{MeV}$ . Discretization effects are also visible for the renormalized Polyakov loop in the low temperature region for p4 and asqtad calculations with  $N_\tau = 8$ . However, the  $N_\tau = 12$  asqtad, HISQ and stout data are all agree. Thus, discretization errors are under control for this quantity.

## 5 Correlation functions of static quark anti-quark pair

One of the most prominent feature of the quark gluon plasma is the presence of chromoelectric (Debye) screening. The easiest way to study chromoelectric screening is to

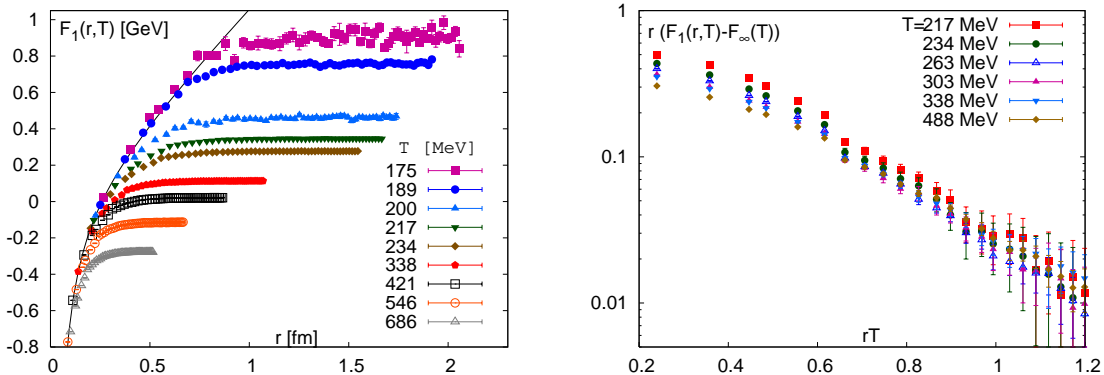


Figure 6: The singlet free energy  $F_1(r, T)$  calculated in Coulomb gauge on  $16^3 \times 4$  lattices (left) and the combination  $F_1(r, T) - F_\infty(T)$  as function of  $rT$  (right). The solid black line is the parametrization of the zero temperature potential.

calculate the singlet free energy of static quark anti-quark pair (for recent reviews on this see Ref. [44, 45]), which is expressed in terms of correlation function of temporal Wilson lines in Coulomb gauge

$$\exp(-F_1(r, T)/T) = \frac{1}{N} \text{Tr}\langle W(r)W^\dagger(0) \rangle. \quad (2)$$

$L = \text{Tr}W$  is the Polyakov loop. Instead of using the Coulomb gauge the singlet free energy can be defined in gauge invariant manner by inserting a spatial gauge connection between the two Wilson lines. Using such definition the singlet free energy has been calculated in  $SU(2)$  gauge theory [46]. It has been found that the singlet free energy calculated this way is close to the result obtained in Coulomb gauge [46]. The singlet free energy turned out to be useful to study quarkonia binding at high temperatures in potential models (see e.g. Refs. [48, 49, 50, 51, 52]). The singlet free energy also appears naturally in the perturbative calculations of the Polyakov loop correlators at short distances [47].

The singlet free energy was recently calculated in QCD with one strange quark and two light quarks with masses corresponding to pion mass of 220 MeV on  $16^3 \times 4$  lattices [53]. The numerical results are shown in Fig. 6. At short distances the singlet free energy is temperature independent and coincides with the zero temperature potential. In purely gluonic theory the free energy grows linearly with the separation between the heavy quark and anti-quark in the confined phase. In presence of dynamical quarks the free energy is saturated at some finite value at distances of about 1 fm due to string breaking [44, 54, 57]. This is also seen in Fig. 6. Above the deconfinement temperature the singlet free energy is exponentially screened at sufficiently large distances [55, 56] with the screening mass proportional to the temperature, i.e.

$$F_1(r, T) = F_\infty(T) - \frac{4}{3} \frac{g^2(T)}{4\pi r} \exp(-m_D(T)r), \quad m_D \sim T. \quad (3)$$

Therefore in Fig. 6 we also show the combination  $F_1(r, T) - F_\infty(T)$  as a function of  $rT$ . As one can see from the figure this function shows an exponential fall-off at distances

$rT > 0.8$ . The fact that the slope is the same for all temperatures means that  $m_D \sim T$ , as expected.

## 6 Temporal meson correlators and spectral functions

Information on hadron properties at finite temperature as well as the transport coefficients are encoded in different spectral functions. In particular the fate of different quarkonium states in QGP can be studied by calculating the corresponding quarkonium spectral functions (for a recent review see Ref. [45]). On the lattice we can calculate correlation function in Euclidean time. This is related to the spectral function via integral relation

$$G(\tau, T) = \int_0^\infty d\omega \sigma(\omega, T) K(\tau, \omega, T), \quad K(\tau, \omega, T) = \frac{\cosh(\omega(\tau - 1/2T))}{\sinh(\omega/2T)}. \quad (4)$$

Given the data on the Euclidean meson correlator  $G(\tau, T)$  the meson spectral function can be calculated using the Maximum Entropy Method (MEM) [58]. For charmonium this was done by using correlators calculated on isotropic lattices [59, 60] as well as anisotropic lattices [61, 62, 63] in the quenched approximation. It has been found that quarkonium correlation function in Euclidean time show only very small temperature dependence [60, 63]. In other channels, namely the vector, scalar and axial-vector channels stronger temperature dependence was found [60, 63]. The spectral functions in the pseudo-scalar and vector channels reconstructed from MEM show peak structures which may be interpreted as a ground state peak [60, 61, 62]. Together with the weak temperature dependence of the correlation functions this was taken as strong indication that the 1S charmonia ( $\eta_c$  and  $J/\psi$ ) survive in the deconfined phase to temperatures as high as  $1.6T_c$  [60, 61, 62]. A detailed study of the systematic effects show, however, that the reconstruction of the charmonium spectral function is not reliable at high temperatures [63], in particular the presence of peaks corresponding to bound states cannot be reliably established. Presence of large cutoff effects at high frequencies also complicates the analysis [66]. The only statement that can be made is that the spectral function does not show significant changes within the errors of the calculations. Recently quarkonium spectral functions have been studied using potential models and lattice data for the singlet free energy of static quark anti-quark pair [50, 51, 52]. These calculations show that all charmonium states are dissolved at temperatures smaller than  $1.2T_c$ , but the Euclidean correlators do not show significant changes and are in fairly good agreement with available lattice data both for charmonium [60, 63] and bottomonium [63, 64]. This is due to the fact that even in absence of bound states quarkonium spectral functions show significant enhancement in the threshold region [49]. Therefore previous statements about quarkonia survival at high temperatures have to be revisited. Exploratory calculations of the charmonium correlators and spectral functions in 2-flavor QCD have been reported in Ref. [65] and the qualitative behavior of the correlation functions was found to be similar.

The large enhancement of the quarkonium correlators above deconfinement in the scalar and axial-vector channel can be understood in terms of the zero mode contribution



[49, 67] and not due to the dissolution of the  $1P$  states as previously thought. Similar, though smaller in magnitude, enhancement of quarkonium correlators due to zero mode is seen also in the vector channel [63]. Here it is related to heavy quark transport [48, 68]. Due to the heavy quark mass the Euclidean correlators for heavy quarkonium can be decomposed into a high and low energy part  $G(\tau, T) = G_{\text{low}}(\tau, T) + G_{\text{high}}(\tau, T)$ . The area under the peak in the spectral functions at zero energy  $\omega \simeq 0$  giving the zero mode contribution to the Euclidean correlator is proportional to some susceptibility,  $G_{\text{low}}^i(\tau, T) \simeq T\chi^i(T)$ , which have been calculated on the lattice in Ref. [69]. It is natural to ask whether the generalized susceptibilities can be described by a quasi-particle model. The generalized susceptibilities have been calculated in Ref. [70] in the free theory. Replacing the bare quark mass entering in the expression of the generalized susceptibilities by an effective temperature dependent masses one can describe the zero mode contribution very well in all channels [69].

While temporal correlators are not sensitive to the change in the spectral functions spatial quarkonium correlation functions could be more sensitive to this. Recent lattice calculations show indication for significant change in spatial charmonium correlators above deconfinement[71].

The spectral function for light mesons has been calculated on the lattice in quenched approximation [72, 74, 75]. However, unlike in the quarkonia case the systematic errors in these calculations are not well understood.

## 7 Conclusions

In recent years significant progress has been achieved in studying strongly interacting matter at high temperatures using lattice QCD. Equation of state and transition temperature have been calculated at several lattice spacings allowing for controlled continuum extrapolations. Current lattice data suggest a transition temperature for chiral symmetry restoration of (150 – 160) MeV. Fluctuations of conserved charges and spatial correlation functions provide detailed picture of the high temperature medium, namely the nature of the relevant degrees of freedom (partonic or hadronic) and color screening. Temporal meson correlation functions have been also studied in lattice QCD but the numerical data are not precise enough to provide detailed information of the corresponding meson spectral functions. However, these lattice data are useful to constrain the model calculations of the meson spectral functions.

## Acknowledgments

This work was supported by U.S. Department of Energy under Contract No. DE-AC02-98CH10886. Computations have been performed using the USQCD resources on clusters at Fermilab and JLab and the QCDOC supercomputers at BNL, as well as the BlueGene/L at the New York Center for Computational Sciences (NYCCS).

## References

- [1] D. Gross, R. Pisarski, L. Yaffe, *Rev. Mod. Phys.* **53**, 43 (1981)
- [2] B. Müller and J. Nagle, *Ann. Rev. Nucl. Part. Sci.* **56**, 93 (2006)
- [3] U. Wiedemann, *Nucl. Phys. A*, **830**, 74c (2009)
- [4] J. Kuti, J. Polónyi and K. Szlachányi, *Phys. Lett. B* **98** (1981) 199;
- [5] L. D. McLerran and B. Svetitsky, *Phys. Rev. D* **24** (1981) 450;
- [6] J. Engels, F. Karsch, H. Satz and I. Montvay, *Phys. Lett. B* **101** (1981) 89.
- [7] G. Boyd *et al.*, *Nucl. Phys. B* **469**, 419 (1996)
- [8] C. W. Bernard *et al.*, [MILC Collaboration], *Phys. Rev. D* **55** (1997) 6861
- [9] A. Ali Khan *et al.*, [CP-PACS Collaboration], *Phys. Rev. D* **64** (2001) 074510
- [10] F. Karsch, E. Laermann and A. Peikert, *Phys. Lett. B* **478** (2000) 447;
- [11] P. Petreczky, *Nucl. Phys. Proc. Suppl.* **140**, 78 (2005);
- [12] E. Laermann and O. Philipsen, *Ann. Rev. Nucl. Part. Sci.* **53**, 163 (2003)
- [13] C. Bernard *et al.* [MILC Collaboration], *Phys. Rev. D* **71**, 034504 (2005)
- [14] Y. Aoki, Z. Fodor, S. D. Katz and K. K. Szabo, *JHEP* **0601**, 089 (2006)
- [15] M. Cheng *et al.*, *Phys. Rev. D* **74**, 054507 (2006)
- [16] Y. Aoki, Z. Fodor, S. D. Katz and K. K. Szabo, *Phys. Lett. B* **643** (2006) 46 [arXiv:hep-lat/0609068].
- [17] C. Bernard *et al.*, *Phys. Rev. D* **75** (2007) 094505
- [18] M. Cheng *et al.*, *Phys. Rev. D* **77** (2008) 014511
- [19] M. Cheng *et al.*, *Phys. Rev. D* **81**, 054504 (2010)
- [20] A. Bazavov *et al.*, *Phys. Rev. D* **80** (2009), 014504
- [21] Y. Aoki, *et al.*, *JHEP* **0906** (2009) 088
- [22] S. Borsanyi *et al.*, [Wuppertal-Budapest Collaboration], arXiv:1007.2580 [hep-lat].
- [23] S. Borsanyi, *et al.*, [Wuppertal-Budapest Collaboration], arXiv:1005.3508 [hep-lat].
- [24] A. Bazavov and P. Petreczky [HotQCD collaboration], *J. Phys. Conf. Ser.* **230**, 012014 (2010);
- [25] A. Bazavov and P. Petreczky [HotQCD Collaboration], *PoS LAT2009*, 163 (2009)

- [26] P. Petreczky, Nucl. Phys. A **830**, 11C (2009)
- [27] C. DeTar and U. M. Heller, Eur. Phys. J. A **41**, 405 (2009);
- [28] Z. Fodor and S. D. Katz, arXiv:0908.3341 [hep-ph];
- [29] P. Petreczky, Eur. Phys. J. ST **155**, 123 (2008)
- [30] K. Orginos, D. Toussaint and R. L. Sugar [MILC Collaboration], Phys. Rev. D **60** (1999) 054503
- [31] P. Huovinen and P. Petreczky, Nucl. Phys. A **837**, 26 (2010)
- [32] P. Huovinen and P. Petreczky, J. Phys. Conf. Ser. **230** (2010) 012012
- [33] J. P. Blaizot, E. Iancu and A. Rebhan, Phys. Rev. Lett. **83** (1999) 2906;
- [34] Phys. Rev. D **63** (2001) 065003
- [35] S.S. Gubser, I.R. Klebanov and I.I Tseytlin, Nucl. Phys. B **534** (1998) 202
- [36] J. O. Andersen, L. E. Leganger, M. Strickland and N. Su, arXiv:1009.4644 [hep-ph].
- [37] M. Cheng *et al.*, Phys. Rev. D **79** (2009) 074505
- [38] J. P. Blaizot, E. Iancu and A. Rebhan, Phys. Lett. B **523** (2001) 143
- [39] A. Rebhan, arXiv:hep-ph/0301130.
- [40] N. Haque and M. G. Mustafa, arXiv:1007.2076 [hep-ph].
- [41] F. Csikor, *et al.*, JHEP **0405** (2004) 046
- [42] P. Petreczky, P. Hegde and A. Velytsky [RBC-Bielefeld Collaboration], PoS **LAT2009**, 159 (2009)
- [43] Y. Aoki, *et al.*, Nature **443**, 675 (2006)
- [44] P. Petreczky, Eur. Phys. J. C **43**, 51 (2005)
- [45] A. Bazavov, P. Petreczky and A. Velytsky, arXiv:0904.1748 [hep-ph].
- [46] A. Bazavov, P. Petreczky and A. Velytsky, Phys. Rev. D **78**, 114026 (2008)
- [47] N. Brambilla, *et. al.*, arXiv:1007.5172 [hep-ph].
- [48] Á. Mócsy and P. Petreczky, Eur. Phys. J. C **43**, 77 (2005);
- [49] Á. Mócsy and P. Petreczky, Phys. Rev. D **73**, 074007 (2006)
- [50] Á. Mócsy and P. Petreczky, Phys. Rev. Lett. **99**, 211602 (2007);
- [51] Á. Mócsy and P. Petreczky, Phys. Rev. D **77**, 014501 (2008);

- [52] Á. Mócsy and P. Petreczky, Eur. Phys. J. ST **155**, 101 (2008)
- [53] RBC-Bielefeld Collaboration, work in progress
- [54] P. Petreczky and K. Petrov, Phys. Rev. D **70**, 054503 (2004)
- [55] O. Kaczmarek et al., Phys. Lett. B **543**, 41 (2002)
- [56] S. Digal, S. Fortunato and P. Petreczky, Phys. Rev. D **68**, 034008 (2003)
- [57] O. Kaczmarek and F. Zantow, Phys. Rev. D **71**, 114510 (2005)
- [58] M. Asakawa, T. Hatsuda and Y. Nakahara, Prog. Part. Nucl. Phys. **46**, 459 (2001)
- [59] S. Datta et al., Nucl. Phys. Proc. Suppl. **119**, 487 (2003)
- [60] S. Datta, *et al.*, Phys. Rev. D **69**, 094507 (2004)
- [61] T. Umeda, K. Nomura and H. Matsufuru, Eur. Phys. J. C **39S1**, 9 (2005)
- [62] M. Asakawa and T. Hatsuda, Phys. Rev. Lett. **92**, 012001 (2004)
- [63] A. Jakovác et al., Phys. Rev. D **75**, 014506 (2007)
- [64] S. Datta, *et al.*, AIP Conf. Proc. **842**, 35 (2006)
- [65] G. Aarts, C. Allton, M. B. Oktay, M. Peardon and J. I. Skullerud, Phys. Rev. D **76**, 094513 (2007)
- [66] F. Karsch, *et al.*, Phys. Rev. D **68**, 014504 (2003) [arXiv:hep-lat/0303017].
- [67] T. Umeda, Phys. Rev. D **75**, 094502 (2007)
- [68] P. Petreczky and D. Teaney, Phys. Rev. D **73**, 014508 (2006)
- [69] P. Petreczky, Eur. Phys. J. C **62**, 85 (2009)
- [70] G. Aarts and J. M. Martinez Resco, Nucl. Phys. B **726** (2005) 93
- [71] S. Mukherjee, Nucl. Phys. A **820** (2009) 283C
- [72] F. Karsch et al., Phys. Lett. B **530**, 147 (2002);
- [73] F. Karsch et al., Nucl. Phys. A **715**, 701 (2003)
- [74] M. Asakawa, T. Hatsuda and Y. Nakahara, Nucl. Phys. A **715**, 863 (2003)
- [75] G. Aarts, et al., Phys. Rev. Lett. **99**, 022002 (2007)